Closed Loop Control of LLC Resonant Converter Incorporating ZVS Boost Converter

N.Madhanakkumar [1], T.S.Sivakumaran[2], G.Irusapparajan [3], D.Sujitha[4]

[1] Research Scholar, Anna University, Tamilnadu, India
[2] Professor, Arunai College of Engineering, India
[3]Professor, [4] PG Scholar, [3,4]Mailam Engineering College, India
[1,2,3,4] Department of Electrical and Electronics Engineering,
[1] nmadhanakkumar@gmail.com [2] sivakumaran1969@gmail.com

Abstract–The modeling and closed loop control of LLC type series-parallel resonant converter is presented in this paper. The LLC resonant converter provides high efficiency with high power density, which leads to their applications in most advance technology. The state – space modeling is analyzed to know the stability of the converter. The common closed loop PI controller is used on both the side of the LLC resonant tank which eliminates the steady-state error and decrease the start-up time of the output voltage. The input of 40V LLC resonant converter is built to produce 220V output with the help of ZVS boost converter. The simulation result is built for this proposed system with 140 kHz resonant frequency. The comparison of simulation result with the open loop and closed loop converter shows the output performance and reliability of a controller.

Keyword – LLC resonant converter, PI controller, ZVS boost converter, State – space modeling.

I. INTRODUCTION

Though various types of resonant converters have abundant preferences in operating with a high switching frequency and low switching losses in that LLC resonant converter which combines the advantages of the SRC and PRC are gaining lots of attention in DC – DC applications.

With the comparison of half-bridge series – resonant (SR), parallel – resonant (PR) and series – parallel resonant converters (SPRC) it is analyzed that SPRC can operate over a wide load range and large input range with excellent efficiency [2]. The optimization of LLC resonant converter is provided with high accuracy and high efficiency with small structure [3, 4, and 6] and used for application such as over current protection [5] with frequency in an acceptable value.

The LLC resonant converter is applicable to various applications of DC – DC converter as SMPS [9], telecommunication [11] and for an adjustable wide range regulated current source [9] with the help of fundamental harmonic approximation method [10]. This FHA analysis cannot explain the practical operation the parasitic components are included with this converter and analyzed with traditional FHA method [7].

The steady – state design is done with the help of state – space modeling method [14, 21] and the state plane trajectories explains about the boundaries of various operating modes [17] for the resonant tank circuit.

II. RESONANT CONVERTER

A. LLC resonant converter:

The LLC resonant converter operates with high power density and high frequency range up to several MHz [12] as it combines the frequencies of SRC and PRC. Though it operates at high frequency the switching losses are reduced and provide high efficient LLC converter design [1].

The LLC resonant converter consists of a resonant capacitor (C_r) and inductor (L_r) in series with the inverter side and another inductor (L_m) in parallel with it to provide high voltage gain [1]. The resonant element C_r and L_r provide series resonant frequency and the combination of L_m and C_r provides parallel resonant frequency.

The LLC resonant converter is one of the type of series – parallel load resonant converter which overcomes the disadvantages of both SRC and PRC as it provides lack in no – load regulation and circulating current independent of load [2] respectively.

The proposed LLC resonant converter consists of four MOSFET switches as full bridge inverter, on the input side or primary side of the transformer under the control of ZVS boost converter.

The output side or secondary side of the transformer consists of four IGBT switches as full bridge rectifier. The LLC resonant converter circuit diagram is shown in Fig.1.

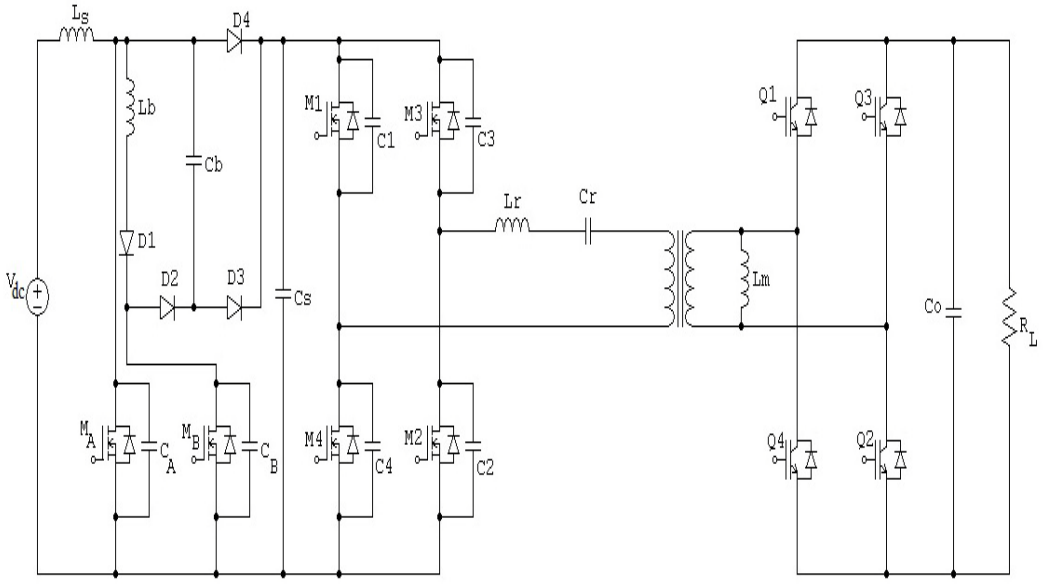

Fig.1. LLC resonant converter circuit diagram.

B. Zero Voltage switching Boost Converter:

As the ZVS is more advantageous than ZCS in the way as ZVS eliminates capacitive turn – on loss, but in ZCS it leads to capacitive turn – on loss with high current loss when operate in high frequency. Thus, ZVS is mostly suitable for high – frequency operation with constant off – time control.

So, in this proposed design to control the input side inverter circuit the ZVS boost converter is applied. The ZVS boost converter works with the principle operation of DC – DC boost converter under zero voltage switching condition of MOSFET switches.

Thus the input voltage of 40Volt is boost up to 150Volt at the output of ZVS boost converter and it acts as input and control the inverter circuit on primary side of the transformer.

III. MODELING ANALYSIS

The modeling is done with the help of state – space modeling. The modeling is used to measure the data for the system model and to predict the system behavior for different input situations. Though there are various techniques for modeling of converter, the state – space modeling is more advantageous than other.

Since, they can be applicable to non – linear, time invariant and MIMO (multiple inputs and multiple outputs) systems it is preferred mostly for modeling of resonant converters. But, the transfer function modeling can be applicable to linear, time invariant system under zero initial conditions.

The state – space modeling is done for the LLC resonant converter in this proposed work based on different mode of operation and with the help of equivalent circuit formation. The state – space matrix is formed only for three modes of operations in this work. The general description of the state – space matrix is given as:

Input Equation: $[dx/dt] = [A][x] + [B][u]$

Output Equation: $[y] = [C][x] + [D][u]$

where, x is the state vector

u is the input

y is the output.

The state vector includes the state variables which is the voltage or current of capacitor or inductor element.

A. State – Space analysis:

Some of the assumptions are made before forming the state – space matrix for above operating modes. The assumptions are:

a) All the components of ZVS boost converter and the components before the inverter side are considered as ideal.
b) The resonant frequency is higher than the switching frequency.
c) The output capacitor is large enough to produce constant output voltage Vo.
d) The circuit losses, including the resonant tank, switch and filter losses are negligible.

1) For PP mode: In PP mode, the switches M_1 and M_2 on the inverter side and T_1 and T_2 on the rectifier side is turned on in positive conduction mode. The state – space input matrix is given as:

$$\begin{bmatrix} \frac{di_r(t)}{dt} \\ \frac{dv_{cr}(t)}{dt} \end{bmatrix} = \begin{bmatrix} 0 & -\frac{1}{L_r} \\ \frac{1}{C_r} & 0 \end{bmatrix} \begin{bmatrix} i_r(t) \\ v_{cr}(t) \end{bmatrix} + \begin{bmatrix} \frac{1}{L_r} \\ 0 \end{bmatrix} [V_{dc} - V_0]$$

and the output equation is,

$$[y] = \begin{bmatrix} 1 & 0 \\ 0 & 1 \end{bmatrix} \begin{bmatrix} i_r \\ v_{cr} \end{bmatrix}$$

2) For PN mode: In this mode of operation, there is a positive conduction of inverter side with the switches M_1 and M_2 turned on and negative conduction on rectifier side with the switches T_3 and T_4 turned on. The state – space input matrix is given as:

$$\begin{bmatrix} \frac{di_r(t)}{dt} \\ \frac{dv_{cr}(t)}{dt} \end{bmatrix} = \begin{bmatrix} 0 & -\frac{1}{L_r} \\ \frac{1}{C_r} & 0 \end{bmatrix} \begin{bmatrix} i_r(t) \\ v_{cr}(t) \end{bmatrix} + \begin{bmatrix} \frac{1}{L_r} \\ 0 \end{bmatrix} [V_{dc} + V_0]$$

and the output equation is,

$$[y] = \begin{bmatrix} 1 & 0 \\ 0 & 1 \end{bmatrix} \begin{bmatrix} i_r \\ v_{cr} \end{bmatrix}$$

3) PO mode: The positive conduction of inverter side with switches M_1 and M_2 turned on and turn off of all the switches on rectifier side defines the PO mode operation. For this mode the state – space input matrix is:

$$\begin{bmatrix} \frac{di_r(t)}{dt} \\ \frac{dv_{cr}(t)}{dt} \end{bmatrix} = \begin{bmatrix} 0 & -\frac{1}{L_r + L_m} \\ \frac{1}{C_r} & 0 \end{bmatrix} \begin{bmatrix} i_r(t) \\ v_{cr}(t) \end{bmatrix} + \begin{bmatrix} \frac{1}{L_r + L_m} \\ 0 \end{bmatrix} [V_{dc}]$$

and the output equation is,

$$[y] = 0$$

B. Stability analysis:

The state – space modeling has one major advantage, as it is used to study about the internal state of the system. Thus, stability of the system using the state – space matrix is found by plotting the bode plot for the whole operation of resonant converter. The equivalent circuit of this resonant converter is shown in Fig.2.

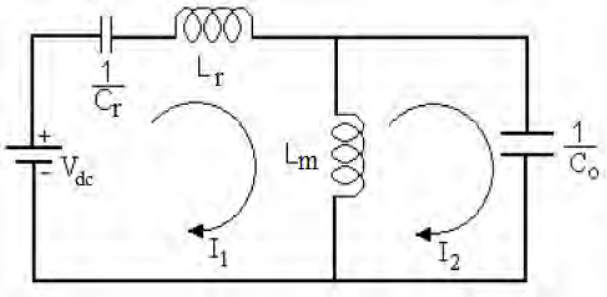

Fig.2. Equivalent circuit of LLC resonant converter

The state – space input matrix for this overall equivalent circuit of LLC resonant converter is given as :

$$\begin{bmatrix} i_1' \\ i_2' \end{bmatrix} = \begin{bmatrix} 0 & 1 \\ -\frac{L_m C_0 + L_m C_1}{L_r L_m C_0} & 0 \end{bmatrix} \begin{bmatrix} i_1 \\ i_2 \end{bmatrix} + \begin{bmatrix} 0 \\ \frac{1}{L_r L_m C_0} \end{bmatrix} [V_{dc}]$$

and the output equation is,

$$[y] = [0 \quad L_1 C_1 C_0] \begin{bmatrix} i_1 \\ i_2 \end{bmatrix}$$

The bode plot for this state – space representation is shown in Fig.3. The stability of the system is used to design the closed loop system. The bode plot shows the magnitude and phase plot for the LLC Resonant converter, from the phase plot it is known that the closed loop system is stable for the chosen LLC values.

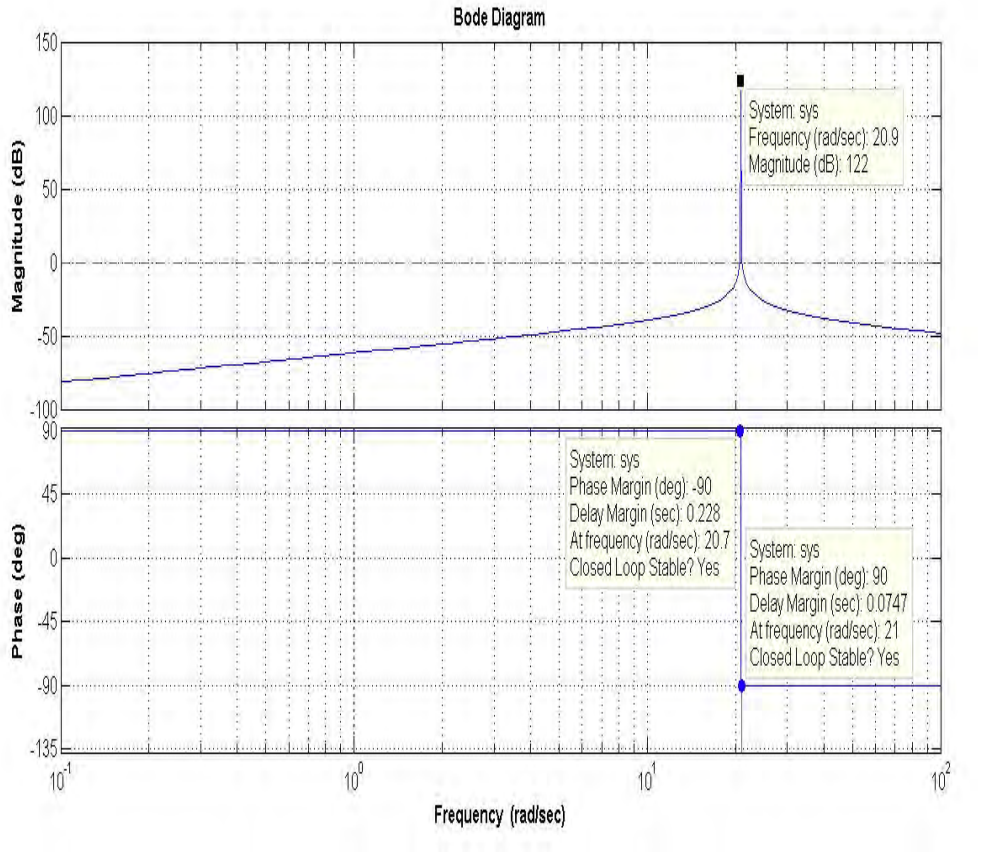

Fig.3. Stability Analysis of LLC Resonant Converter Using Bode Plot

IV. DESIGN OF CLOSED LOOP PI CONTROL

The closed loop PI control method is designed such as giving the control signal to ZVS boost converter and rectifier side of LLC resonant converter. The block diagram representation of this proposed work is shown in Fig.4.

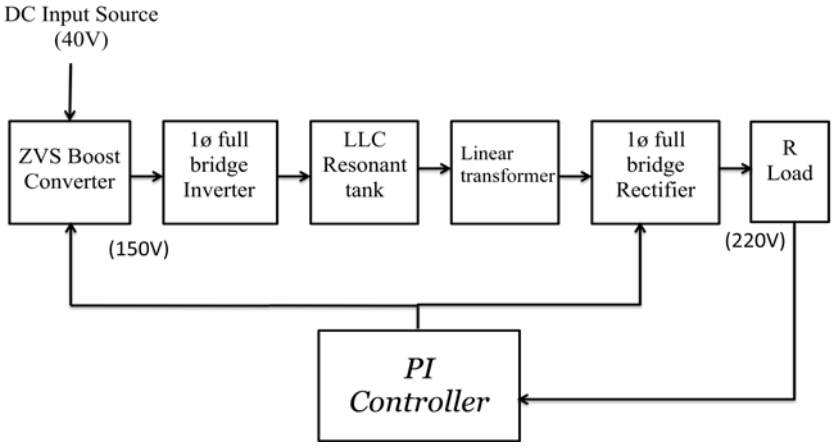

Fig.4. Block Diagram of closed loop LLC resonant converter

The common PI controller is used to give control signals on both the side of resonant tank and linear transformer. In this closed loop system, the system error is reduced using trial and error method of PI controller.

The PI controller is a special case of controller, which is used in abundant for controlling the system. The PI controller has proportional and integral error, but derivative (D) of the error is not used, since it is more sensitive to high frequencies in the input side.

A. Proportional term:

The proportional term produces an output value that is proportional to current error value. The response of the output is improved by multiplying the proportional constant K_P with the error value.

B. Integral term:

The integral term is proportional to both the magnitude of the error and the duration of the error. The response of the output is improved by multiplying the integral constant K_I with the accumulated error value. Thus, PI controller is used to reduce the rise time and also eliminates the steady – state error to improve the output of the system.

V. SIMULATION RESULTS

The Fig.5.1 and 5.2 shows the closed loop responses of LLC resonant converter start – up output voltage and current with set point of 40V and nominal load of 100Ω. The Fig.5.3 and 5.4 shows their responses of output voltage and current respectively under sudden line disturbance (40V – 42V – 40V) at 0.8sec with nominal load of 100Ω and Fig.5.5 and 5.6 shows their responses of output voltage and current under sudden load disturbance (100 Ω – 90 Ω – 100 Ω) at 0.5sec with set point of 40V respectively with PI controller.

Similarly, the open loop responses for the performance comparison of closed loop control with open loop control are shown from Fig.5.7 – Fig.5.12. The Fig.5.7 and 5.8 shows the open loop responses of LLC resonant converter start – up output voltage and current with set point of 40V and nominal load of 100Ω. The Fig.5.9 and 5.10 shows their responses of output voltage and current respectively under sudden line disturbance (40V – 42V – 40V) at 0.8sec with nominal load of 100Ω and figure 5.11 and 5.12 shows their responses of output voltage and current under sudden load disturbance (100 Ω – 90 Ω – 100 Ω) at 0.5sec with set point of 40V respectively.

With these simulation results, the comparison TABLE I is drawn to clearly predict the performance of the LLC resonant converter and the controller importance in the system. The TABLE I show the performance of LLC resonant converter under open loop and closed loop control. The TABLE II shows the parameter specifications for LLC resonant converter. The Fig.5.13 shows the graphical comparison of simulated performances of open loop and closed loop system for LLC Resonant converter.

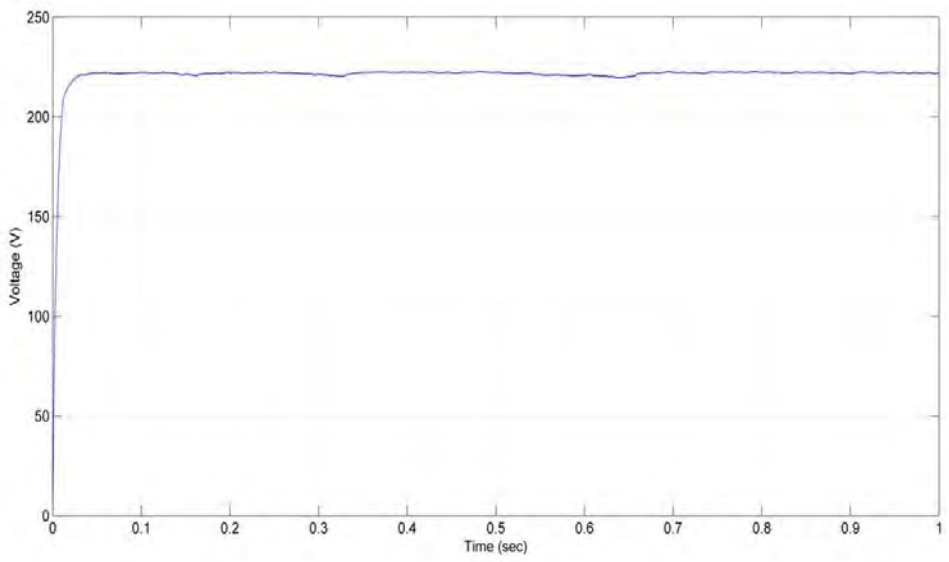

Fig.5.1 Simulated start-up voltage of LLCRC with set - point 40V and nominal load 100Ω (PI Controller)

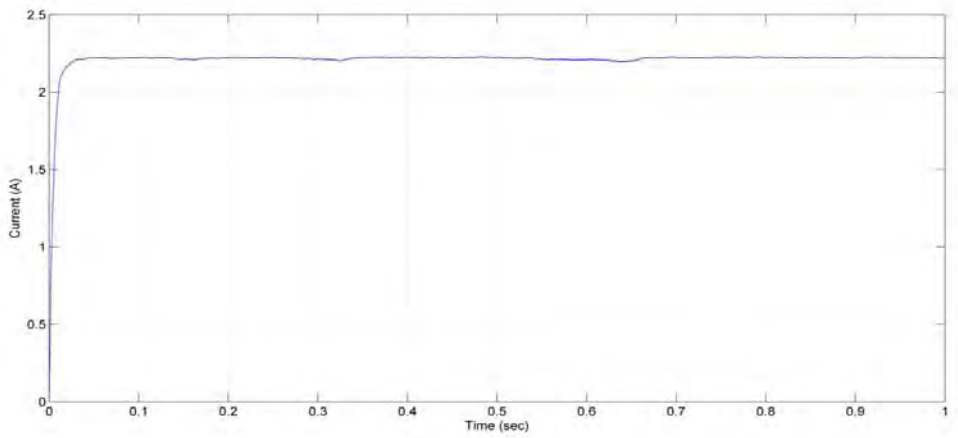

Fig.5.2. Simulated start-up current of LLCRC with set - point 40V and nominal load 100Ω (PI Controller)

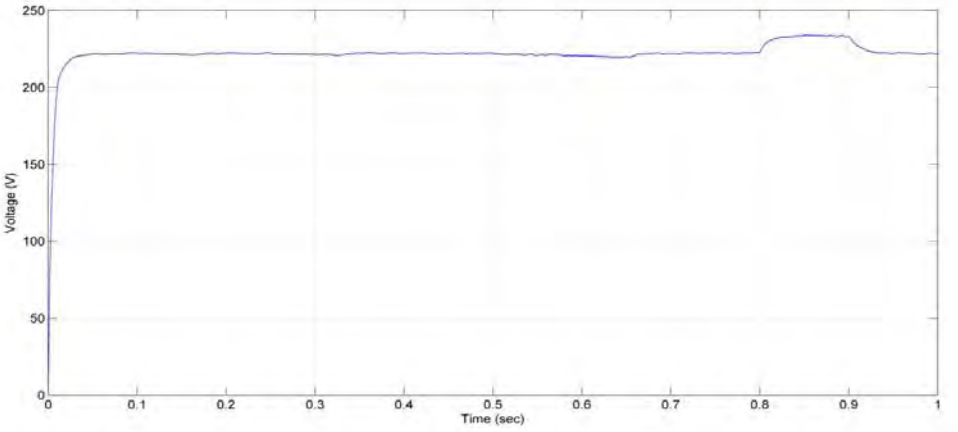

Fig.5.3. Simulated output voltage of LLCRC with sudden line disturbances (40V – 42V – 40V) at t = 0.8sec (PI Controller)

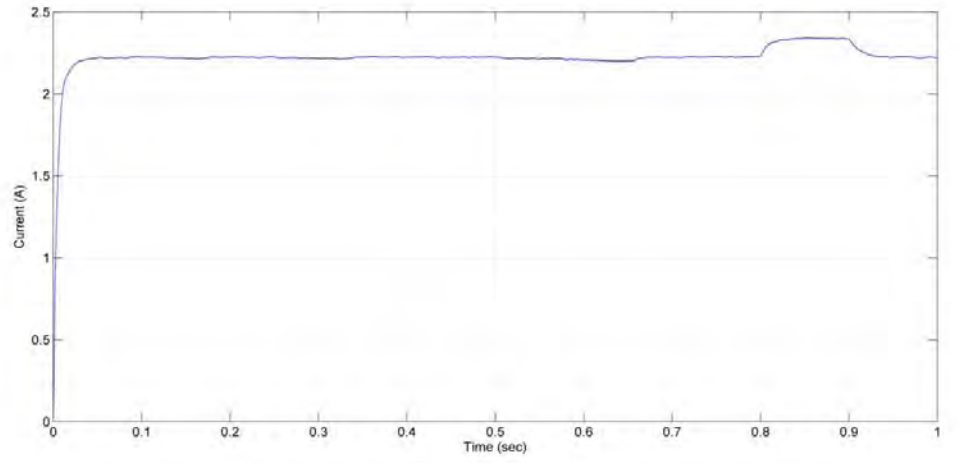

Fig.5.4. Simulated output current of LLCRC with sudden line disturbances (40V – 42V – 40V) at t=0.8sec (PI Controller)

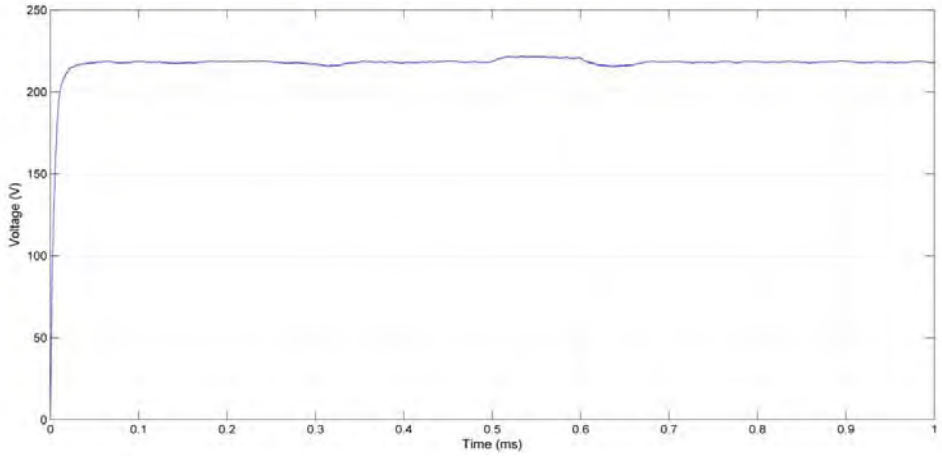

Fig.5.5. Simulated output voltage of LLCRC with sudden load disturbances (100Ω – 90 Ω – 100Ω) at t=0.5sec (PI Controller)

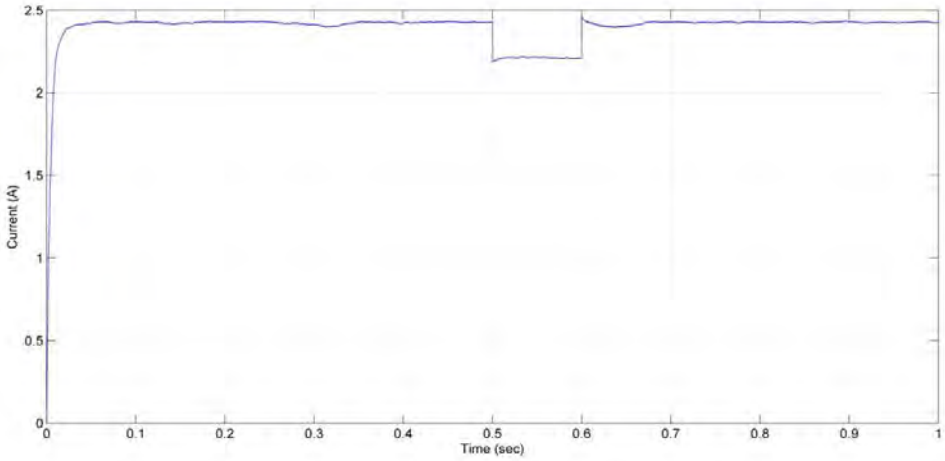

Fig.5.6. Simulated output current of LLCRC with sudden load disturbances (100Ω – 90 Ω – 100Ω) at t=0.5sec (PI Controller)

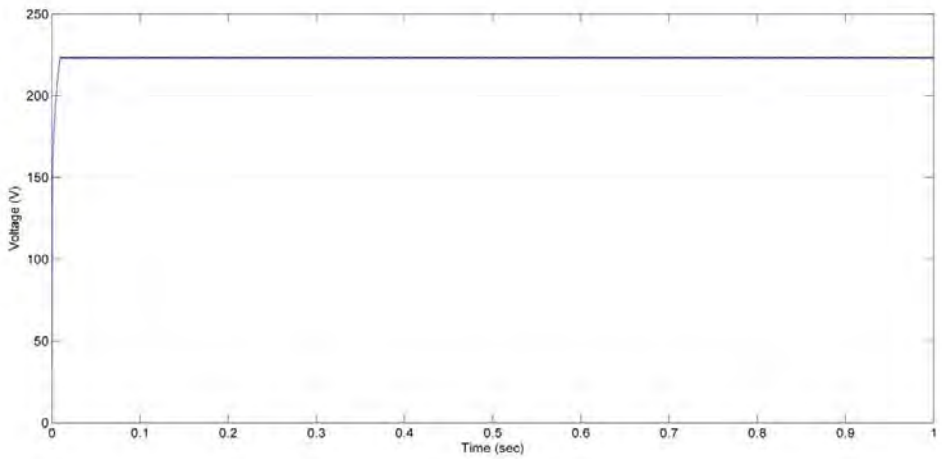

Fig.5.7. Simulated start-up voltage of LLCRC with set - point 40V and nominal load 100Ω (Open Loop)

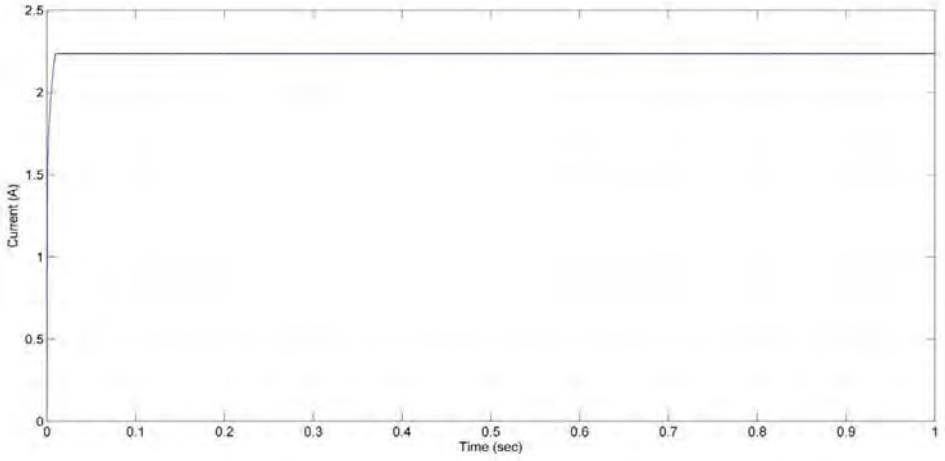

Fig.5.8. Simulated start-up current of LLCRC with set - point 40V and nominal load 100Ω (Open Loop)

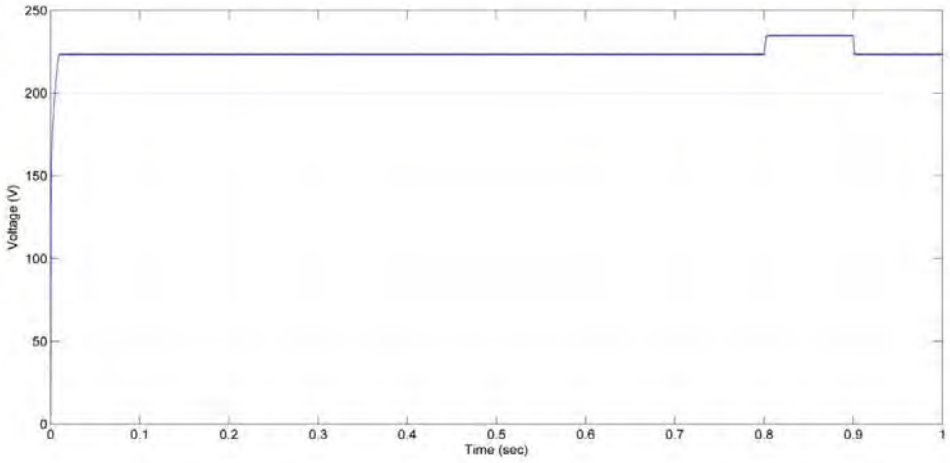

Fig.5.9. Simulated output voltage of LLCRC with sudden line disturbances (40V – 42V – 40V) at t=0.8sec (Open Loop)

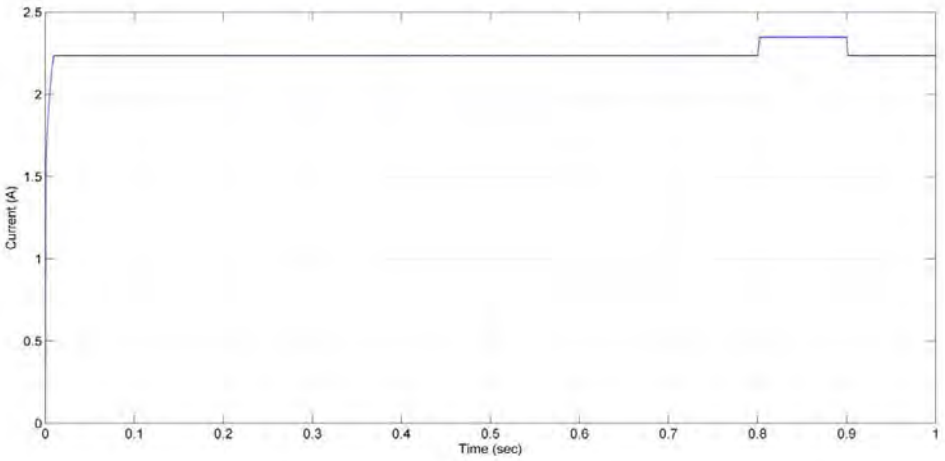

Fig.5.10. Simulated output current of LLCRC with sudden line disturbances (40V – 42V – 40V) at t=0.8sec (Open Loop)

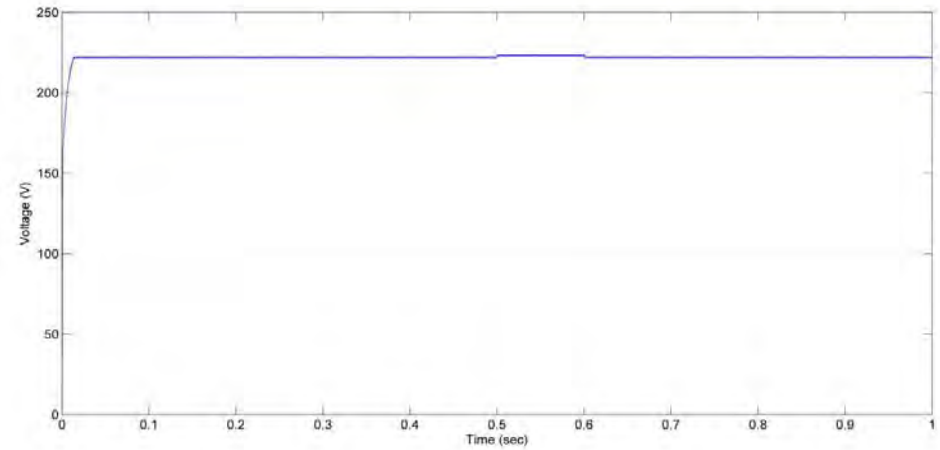

Fig.5.11. Simulated output voltage of LLCRC with sudden load disturbances (100Ω – 90 Ω – 100Ω) at t=0.5sec (Open Loop)

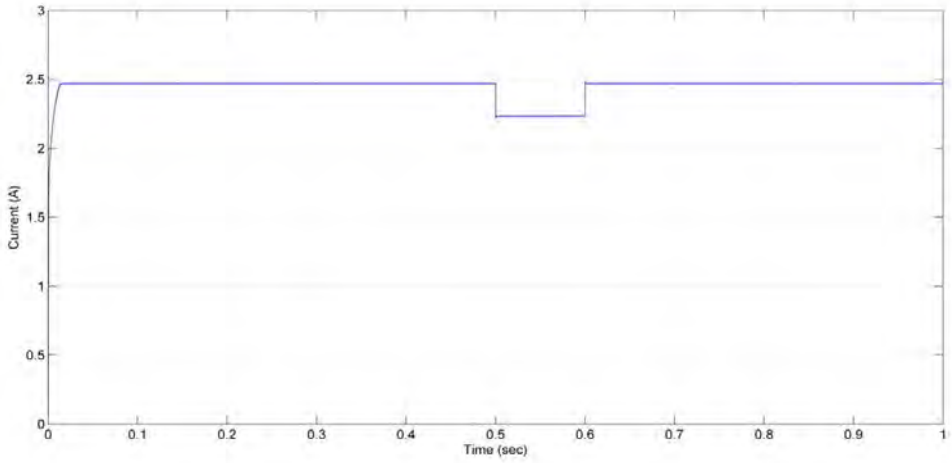

Fig.5.12. Simulated output current of LLCRC with sudden load disturbances (100Ω – 90 Ω – 100Ω) at t=0.5sec (Open Loop)

TABLE I
Performance Evaluation of Open Loop LLC Resonant Converter with Closed Loop Control

LLC Resonant Converter	Start – up Transient 40 V			Supply Disturbance Increase – 2 V			Load Disturbance Decrease – 10Ω		
	Delay time (sec)	Rise time (sec)	Settling time (sec)	Delay time (sec)	Rise time (sec)	Settling time (sec)	Delay time (sec)	Rise time (sec)	Settling time (sec)
Closed Loop	0.000412	0.00856	0.0121	0.00412	0.008462	0.01181	0.000412	0.02126	0.01252
Open Loop	0.00317	0.01463	0.03474	0.003172	0.01644	0.04299	0.00318	0.0332	0.01599

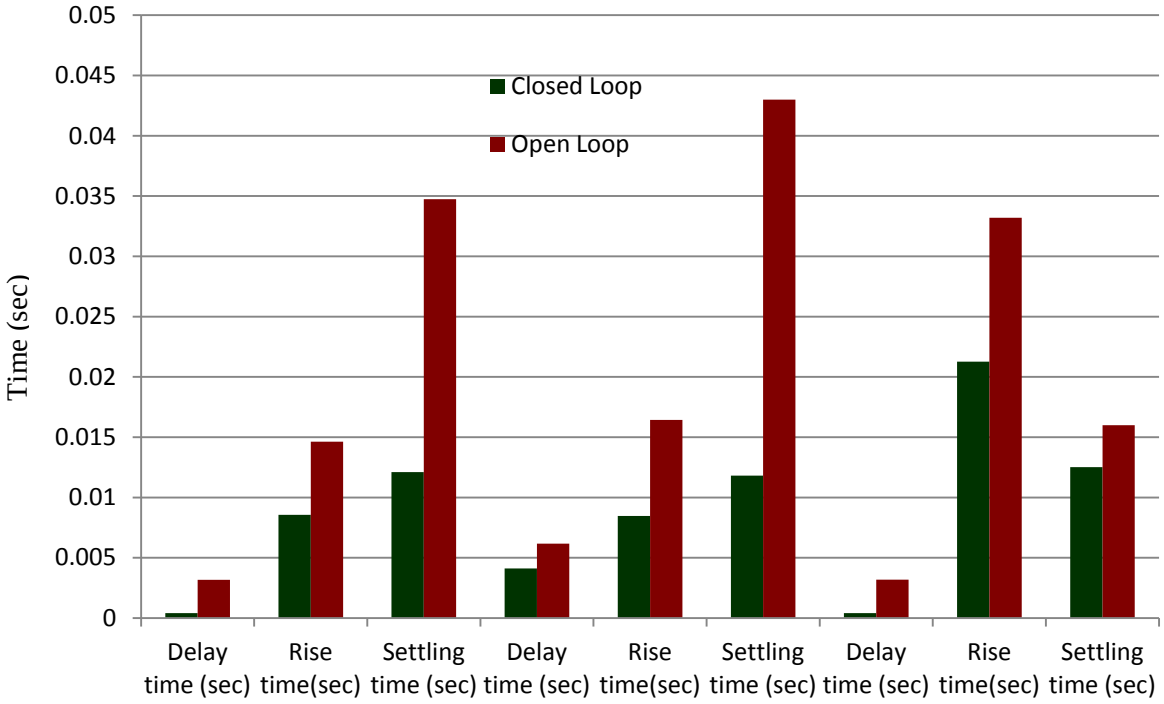

Fig. 5.13 Graphical comparison of simulated performances of open loop and closed loop system for LLCRC

TABLE II
Parameters Specification for LLC Resonant Converter

Parameters	Values
Input Voltage, V_s	40V
Resonant Capacitor, C_r	470nF
Resonant Inductor, L_r	2.75μH
Load Resistance, R_L	100 Ω
Resonant Inductor, L_m	7.67μH
Output Voltage, V_o	220V

VI. CONCLUSION

Thus, the closed loop control of LLC resonant converter performance was obtained using PI controller. The simulation result with reduced rise – time and elimination of steady – state error was obtained. The system performed well under sudden load disturbance. The stability of the system was also analyzed with the help of bode plot and state – space analysis. The open loop and closed loop characteristic performance was compared and shows that the closed loop control is less sensitive to the disturbances than open loop system.

REFERENCES

[1] Xiang Fang, Haibing Hu, Frank Chen, Utsav Somani, Emil Auadisian, John Shen, and Issa Batarseh, "Efficiency – oriented optimal design of the LLC resonant converter based on peak gain placement", in Proc. IEEE Trans. on Power Electron., Vol. 28, No. 5, May 2013.

[2] R. L. Steigerwald, "A comparison of half-bridge resonant converter topologies," IEEE Trans. Power Electron. , vol. 3, no. 2, pp. 174–182, Apr. 1988.

[3] T. Liu, Z. Zhou, A. Xiong, J. Zeng, and J. Ying, "A novel precise design method for LLC series resonant converter," in Proc. 28th Annul. Int. Telecomm. Energy Conf.,2006, pp.1-6.

[4] C. Oeder, "Analysis and design of a low-profile LLC converter," in Proc. IEEE Int. Symp. Ind. Electron. , Jul. 2010, pp. 3859–3864.

[5] X. Xie, J. Zhang, C. Zhao, Z. Zhao, and Z. Qian, "Analysis and optimization of LLC resonant converter with a novel over-current protection circuit," IEEE Trans. Power Electron., vol. 22, no. 2, pp. 435–443, Mar. 2007.

[6] M. P. Foster, C. R. Gould, A. J. Gilbert, D. A. Stone, and C. M. Bingham, "Analysis of CLL voltage-output resonant converters using describing functions," IEEE Trans. Power Electron., vol. 23, no. 4, pp. 1772–1781, Jul. 2008.

[7] B. Lee, M. Kim, C. Kim, K. Park, and G. Moon, "Analysis of LLC resonant converter considering effects of parasitic components," in Proc. IEEE Int. Telecomm. Energy Conf., Oct. 2009, pp. 1–6.

[8] G. Ivensky, S. Bronshtein, and A. Abramovitz, “Approximate analysis of resonant LLC DC–DC converter,” IEEE Trans. Power Electron., vol. 26, no. 11, pp. 3274–3284, Nov. 2011.
[9] R. Beiranvand, B. Rashidian, M. R. Zolghadri, and S. M. H. Alavi, “Designing an adjustable wide range regulated current source,” IEEE Trans. Power Electron., vol. 25, no. 1, pp. 197–208, Jan. 2010.
[10] T. Duerbaum, “First harmonic approximation including design constraints,” in Proc. 20th Int. Telecommun. Energy Conf.,, 1998, pp. 321–328.
[11] W.-Y. Choi, J.-M. Kwon, and B.-H. Kwon, “High-performance front-end rectifier system for telecommunication power supplies,” Proc. Inst. Elect. Eng., vol. 153, no. 4, pp. 473–482, 2006.
[12] H. de Groot, E. Janssen, R. Pagano, and K. Schetters, “Design of a 1-MHz LLC resonant converter based on a DSP-Driven SOI Half-Bridge power MOS module,” IEEE Trans. Power Electron., vol. 22, no. 6, pp. 2307–2320, Nov. 2007.
[13] B. Yang, F. C. Lee, A. J. Zhang, and G. Huang, “LLC resonant converter for front end DC/DC conversion,” in Proc. IEEE Appl. Power Electron. Conf. Expo., 2002, pp. 1108–1112.
[14] J. H. Cheng and A. F. Witulski, “Analytic solutions for LLCC parallel resonant converter simplify use of two-and three-element converters,” IEEE Trans. Power Electron., vol. 13, no. 2, pp. 235–243, Mar. 1998.
[15] X. Fang, H. Hu, J. Shen, and I. Batarseh, “Operation mode analysis and peak gain approximation of the LLC resonant converter,” IEEE Trans. Power Electron., vol. 27, no. 4, pp. 1985–1995, Apr. 2012.
[16] B. Lu, W. Liu, Y. Liang, F. C. Lee, and J. D. van Wyk, “Optimal design methodology for LLC resonant converter,” in Proc. IEEE Appl. Power Electron. Conf. Expo., Mar. 2006, vol. 2, p. 6.
[17] N. H. Kutkut, C. Q. Lee, and I. Batarseh, “A generalized program for extracting the control characteristics of resonant converters via the state - plane diagram,” IEEE Trans. Power Electron., vol. 13, no. 1, pp. 58–66, Jan. 1998.
[18] I. Batarseh, “State-plane approach for the analysis of half-bridge parallel resonant converters,” Proc. Inst. Elect. Eng., vol. 142, no. 3, pp. 200–204, Jun. 1995.
[19] A. K. S. Bhat, “A generalized steady-state analysis of resonant converters using two-port model and Fourier-series approach,” IEEE Trans. Power Electron, vol. 13, no. 1, pp. 142–151, Jan. 1998.
[20] I. Batarseh, R. Liu, A. Ortiz-Conde, A. Yacoub, and K. Siri, “Steady state analysis and performance characteristics of the LLC-type parallel resonant converter,” in Proc. Power Electron. Spec. Conf., 1994, pp. 597–606.
[21] J. F. Lazar and R. Martinelli, “Steady-state analysis of the LLC series resonant converter,” in Proc. IEEE Appl. Power Electron. Conf. Expo., 2001, vol. 2, pp. 728–735.
[22] Y. Gu, Z. Lu, L. Hang, Z. Qian, and G. Huang, “Three-level LLC series resonant DC/DC converter,” IEEE Trans. Power Electron., vol. 20, no. 4, pp. 781–789, Jul. 2005.
[23] C. Nagarajan, M. Muruganandam, D. Ramasubramanian, “Analysis and Design of CLL Resonant Converter for Solar Panel-battery Systems,” I.J. Intelligent Systems and Applications, Jan. 2013, pp. 52-58.